Removal of sedimentation decreases relative deposition of coarse particles in the lung periphery

C. Darquenne, K. L. Zeman, R. C. Sá, T. K. Cooper, J. M. Fine, W. D. Bennett and G. K. Prisk

J Appl Physiol 115:546-555, 2013. First published 6 June 2013;
doi: 10.1152/japplphysiol.01520.2012

Journal of Applied Physiology publishes original papers that deal with diverse area of research in applied physiology, especially those papers emphasizing adaptive and integrative mechanisms. It is published 24 times a year (twice monthly) by the American Physiological Society, 9650 Rockville Pike, Bethesda MD 20814-3991.
 ESSN: 1522-1601. Visit our website at http://www.the-aps.org/.

J Appl Physiol 115: 546–555, 2013.
First published June 6, 2013; doi:10.1152/japplphysiol.01520.2012.

Removal of sedimentation decreases relative deposition of coarse particles in the lung periphery

C. Darquenne,[1] K. L. Zeman,[2] R. C. Sá,[1] T. K. Cooper,[3] J. M. Fine,[1] W. D. Bennett,[2] and G. K. Prisk[1,3]

[1]*Department of Medicine, University of California, San Diego, La Jolla, California;* [3]*Department of Radiology, University of California, San Diego, La Jolla, California;* [2]*Department of Medicine, University of North Carolina at Chapel Hill, Chapel Hill, North Carolina*

Submitted 20 December 2012; accepted in final form 31 May 2013

Darquenne C, Zeman KL, Sá RC, Cooper TK, Fine JM, Bennett WD, Prisk GK. Removal of sedimentation decreases relative deposition of coarse particles in the lung periphery. *J Appl Physiol* 115: 546–555, 2013. First published June 6, 2013; doi:10.1152/japplphysiol.01520.2012.—Lung deposition of >0.5-μm particles is strongly influenced by gravitational sedimentation, with deposition being reduced in microgravity (μG) compared with normal gravity (1G). Gravity not only affects total deposition, but may also alter regional deposition. Using gamma scintigraphy, we measured the distribution of regional deposition and retention of radiolabeled particles (^{99m}Tc-labeled sulfur colloid, 5-μm diameter) in five healthy volunteers. Particles were inhaled in a controlled fashion (0.5 l/s, 15 breaths/min) during multiple periods of μG aboard the National Aeronautics and Space Administration Microgravity Research Aircraft and in 1G. In both cases, deposition scans were obtained immediately postinhalation and at 1 h 30 min, 4 h, and 22 h postinhalation. Regional deposition was characterized by the central-to-peripheral ratio and by the skew of the distribution of deposited particles on scans acquired directly postinhalation. Relative distribution of deposition between the airways and the alveolar region was derived from data acquired at the various time points. Compared with inhalation in 1G, subjects show an increase in central-to-peripheral ratio ($P = 0.043$), skew ($P = 0.043$), and tracheobronchial deposition ($P < 0.001$) when particles were inhaled in μG. The absence of gravity caused fewer particles to deposit in the lung periphery than in the central region where deposition occurred mainly in the airways in μG. Furthermore, the increased skew observed in μG likely illustrates the presence of localized areas of deposition, i.e., "hot spots", resulting from inertial impaction. In conclusion, gravity has a significant effect on deposition patterns of coarse particles, with most of deposition occurring in the alveolar region in 1G but in the large airways in μG.

gravity; human lung; gamma scintigraphy; aerosol retention

THE TOXICITY OF INHALED PARTICLES not only depends on the sites of deposition in the lung, but also on how fast deposited particles can be removed or translocated. Particles that deposit in the conducting airways are mainly removed by mucociliary clearance, while most of the particles that deposit in the alveolar region are phagocytized and cleared by alveolar macrophages. The rate of these clearance mechanisms differs by several orders of magnitude, with mucociliary clearance being very much the faster process (half-life of hours/day vs. months/years) (34, 39). Thus small changes in aerosol deposition location have the potential to result in substantial differences in retention periods of inhaled aerosols and hence exposure.

Address for reprint requests and other correspondence: C. Darquenne, Dept. of Medicine, UCSD, 9500 Gilman Dr., mail code 0623A, La Jolla, CA 92093-0623 (e-mail: cdarquenne@ucsd.edu).

Planar gamma scintigraphy is the most widely used radionuclide imaging method to assess regional aerosol deposition and retention in the human lung. The most common analysis divides the lung into a central (C) and peripheral (P) region from which regional lung distribution of deposited particles can be derived through the C-to-P ratio (C/P). It should be noted that, because of the two-dimensional (2D) nature of the imaging technique, while most of the large and many of the intermediate airways are included in the C region defined on the planar images, the C region also includes a significant portion of the lung parenchyma, confounding the estimation of deposition in the central airways (36). By measuring the retention of deposited particles over a 24-h period following aerosol inhalation, one can assess the distribution of deposited particles in the conducting airways and the lung parenchyma, assuming that particles deposited in the conducting airways are removed only by mucociliary clearance with no long-term retention component (28, 36, 42). Indeed, it has been generally accepted that insoluble particles that deposited in the lung are cleared during two general phases. The first phase, identified as "tracheobronchial," has clearance half-times between 6 and 12 h and concludes by convention after 24 h (22, 41). The second phase, identified as "alveolar," requires several months to years to complete.

Previous studies by our group (12, 14, 16, 17) have shown that the deposition of particles larger than 0.5 μm in diameter in the lung is strongly influenced by gravitational sedimentation. While deposition is lowered by reduced gravity, the reduced sedimentation means that fewer particles deposit in the airways, increasing the number of particles transported to the lung periphery. In the case of 1-μm particles, this results in a more peripheral site of deposition, as measured by the aerosol bolus technique (14). As a result, not only total deposition, but also regional deposition may be affected by gravity. These changes in aerosol deposition location can potentially result in substantial differences in retention periods of inhaled aerosols. If particles were to be mainly deposited centrally in the absence of gravity, their residence time in the lungs would be reduced. Conversely, if particles were to be deposited more peripherally in microgravity (μG) than in normal gravity (1G) then they would not be readily cleared by the mucociliary clearance system, thus increasing their residence time in the lungs. This could be a concern for future space explorations to other planetary bodies. For example, the dust present on the surface of the Moon has a significant fraction in the inhalable range (24) and is thought to be highly reactive in nature due to exposed surfaces analogous to terrestrial fresh-fractured quartz, a substance with potent toxicological properties. Therefore, it is important to

understand the mechanisms by which particles that do penetrate in the lung and deposit in low gravity are cleared (31).

Few existing models of aerosol deposition in the human lung have examined the effect of gravity on aerosol deposition. Using a five-lobe model of the human lung, Asgharian et al. (1) studied the effect of gravity on airflow distribution and particle deposition in the lung. For resting conditions (flow rate of 250 ml/s and tidal volume of 675 ml), they predicted lower overall deposition in μG than in 1G for both 1- and 10-μm particles. They also found that, while deposition in the large and intermediate conducting airways were relatively unaffected by gravity, alveolar deposition was significantly reduced in the absence of gravity, especially for coarse particles (≥5 μm). Using a one-dimensional model of the human lung, Darquenne and colleagues (12) also predicted lower deposition in μG compared with 1G, although no predictions on the effect of gravity on regional deposition was provided. Finally, using more complex models of the acinar regions, Ma and Darquenne (32) predicted a much-reduced deposition in μG compared with 1G for coarse particles. These predictions suggest that C/P, as measured by gamma scintigraphy, should be increased, and a greater fraction of deposited particles cleared in 22 h in μG because of a reduction of long-resident P deposition.

In our laboratory's previous studies in altered gravity (12, 14, 16, 17), aerosol deposition was determined using photometer techniques that did not provide information on the spatial location of deposited particles. Such information is essential for determining particle retention rates in the lung and is the focus of this study. Using planar gamma scintigraphy, we measured the retention rates of insoluble radiolabeled particles with a mass median average diameter (MMAD) of ~5 μm that was inhaled and deposited in healthy humans, both on the ground (1G) and in μG during parabolic flights. For both in-flight (μG) and ground measurements, deposition and retention of particles were determined by planar gamma scintigraphy immediately following particle inhalation, and at 1 h 30 min, 4 h, and 22 h postdeposition. The data showed that gravity has a significant effect on deposition patterns of coarse particles, with most of the deposition occurring in the alveolar region in 1G, but in the bronchial airways in μG.

METHODS

Subjects and protocol. Six healthy subjects were enrolled in the study, and complete data sets were obtained on five. None of the subjects was a smoker or had a history of pulmonary disease. Relevant anthropometric data of subjects who completed the study are listed in Table 1. Because some of them also participated in previous studies aboard the National Aeronautics and Space Administration (NASA) Microgravity Research Aircraft (11–14, 16, 17), we retained their subject numbers for comparison purposes. The subjects were permitted to take anti-motion sickness medication provided by NASA (scopolamine and dextra-amphetamine in a body weight-based dose), and none exhibited symptoms of motion sickness in flight. Subjects who took anti-motion sickness medication during flight were required to take the same dose with the same timing in the delayed synchronous ground control studies. The study was approved by the Human Research Protection Program at the University of California at San Diego, by the Committee on the Protection of the Rights of Human Subjects at the University of North Carolina, and by the Institutional Review Board at the Johnson Space Center, Houston, TX. Written, informed consent was obtained from each participant before the start of the studies.

Table 1. *Anthropometric data*

Subject No.	Sex	Age, yr	Height, cm	Weight, kg	FEV_1, %predicted	FEV_1/FVC, %predicted
1	F	44	165	57	104	96
8	F	47	174	83	83	110
10	M	36	178	85	85	101
11	M	59	178	70	116	104
14	M	49	175	92	87	107

F, female; M, male; FEV_1, forced expiratory volume in 1 s; FVC, forced vital capacity.

Data were obtained by measuring retention rates of Technetium-99 (^{99m}Tc) radiolabeled sulfur-colloid particles that were deposited in the lung during periods of μG in the NASA Reduced Gravity Aircraft and on the ground in 1G, in the seated posture. Each subject was studied on two occasions, each separated by at least 48 h. Aerosol delivery was first performed in μG and then on the ground (on a second occasion), where timing of aerosol delivery was matched to the timing of aerosol delivery during parabolic flight. Subjects breathed either filtered air or air containing labeled particles via a mouthpiece while seated in front of a 40-cm gamma camera head (MiE America, Chicago, IL) (Fig. 1*A*). The aerosol delivery system allowed for rapid activation and deactivation of the particle supply so that subjects were only exposed to particles during the μG phase of the parabolic flight, and breathed particle-free air at all other times. Subjects controlled their ventilation using an audible electronic metronome and a flowmeter to target a flow rate of 0.5 l/s and an inspiratory and expiratory time of 2 s, resulting in a tidal volume of ~1 liter, as used in previous studies (12, 19). Particle delivery occurred during multiple separate periods of μG until the deposited dose reached ~40 μCi, as monitored by the gamma camera. About 8 s before the end of each μG period of particle inhalation, particle generation was terminated, and subjects exhaled fully to residual volume to clear the air in the lungs of as many airborne particles as possible before transition to the hypergravity phase of the parabola, so that aerosol deposition during hypergravity could be minimized (Fig. 1*B*). Following inhalation of the radiolabeled particles, gamma scintigraphy was used to determine retention rates (5, 19) by acquiring multiple timed images of activity in the lung fields.

Aerosol generation. Radiolabeled (^{99m}Tc, 10 mCi/370 MBq) sulfur colloid (SC) particles were prepared from CIS-Sulfur Colloid kits (CIS-US), following the procedure provided by the manufacturer. The ^{99m}Tc-SC particles were obtained in a liquid suspension and had a mean diameter of 0.22 μm and a GSD (geometric standard deviation) of 1.75. The suspension was mixed with saline and nebulized into an aerosol with a vibrating mesh nebulizer, the Aeroneb (Aeroneb Laboratories, Nektar, San Carlos, CA). The nebulizer was placed in line with the subject's breathing path and was shielded in a lead container with minimal dead space between its output and the mouthpiece to the subject to minimize evaporation of particles before inhalation. A high-efficiency filter was located on the distal side of the nebulizer to capture exhaled particles.

Measurements using a Sierra Series 210 eight-stage cascade impactor (Sierra Instruments, Carmel Valley, CA) showed a size of 4.9 μm (MMAD) with a GSD of 2.5 in 1G and a MMAD of 5.6 μm with a GSD of 2.4 in μG.

Gamma scintigraphy. Before each study, while on the ground, the subject was seated with his/her back to the gamma camera, and a lung transmission scan of ~90 s was recorded by placing a planar solid sheet containing the radioisotope Co-57 (<25 mCi) in front of the subject. The scan was used to determine whole lung outlines and regions of interest (ROIs) for characterizing relative regional deposition and clearance in the lung. Background images of the subject were

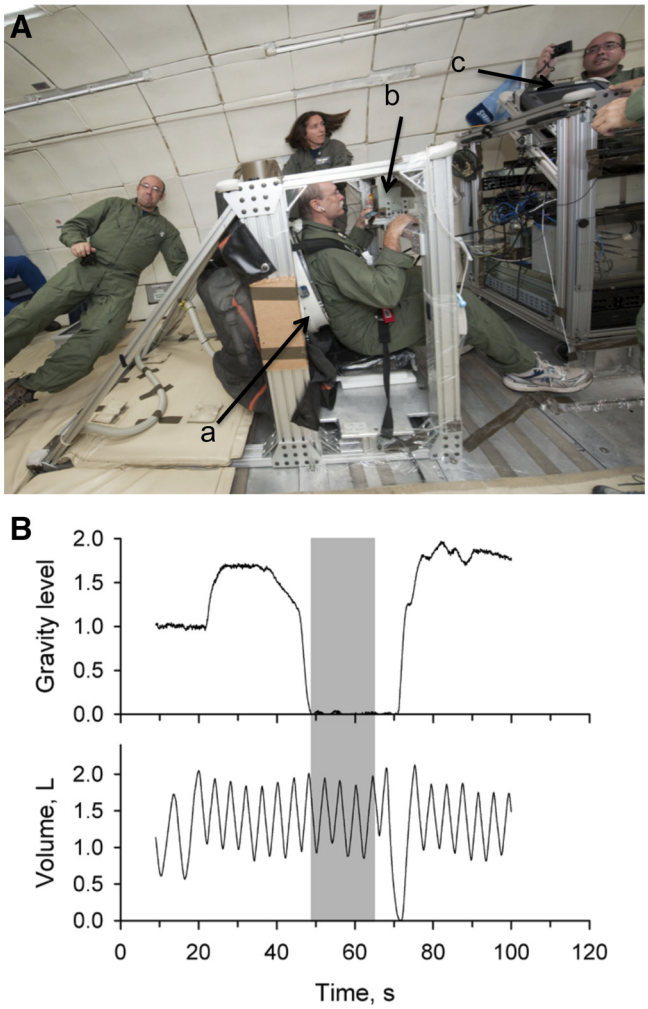

Fig. 1. Configuration of the equipment aboard the National Aeronautics and Space Administration (NASA) Microgravity Research Aircraft during data collection and typical timeline of aerosol delivery. *A*: equipment. A subject was seated in front of the gamma camera (*a*) and strapped with seat belts to minimize subject motion during the different phase of the parabolic flights. A lead box containing the aerosol nebulizer (*b*) was positioned in front of the subject. Deposition of aerosol was monitored throughout the experiment and displayed on monitor screen (*c*). (Photo courtesy of NASA). *B*: typical tracings of gravity level and respired volume during parabolic flight. Shaded area indicates period during which aerosol was delivered to the subject. Note that, immediately following termination of aerosol generation, subject exhaled to residual volume before the start of the hypergravity phase.

taken before both the transmission scan and radiolabeled aerosol inhalation.

For each study (ground/in-flight), the subject inhaled the ^{99m}Tc-SC aerosol while seated in front of the gamma camera. Immediately following exposure, an initial deposition scan of ~10 min was recorded. Images were then recorded for a 15-min period at 1 h 30 min postdeposition and for 30 min at 4 h and ~22 h postdeposition. For all imaging sessions, the subject had two small fiduciary point sources of Americium (^{241}Am, <1 μCi) placed in a standard location on the subject's back (along the spine and outside of the lung field) to ensure accurate matching of the images taken at the various times postdeposition. Subjects were freely breathing at their resting tidal volume during the imaging sessions that were all performed on the ground in 1G, except for the initial deposition scan of the flight studies that was recorded during flight and, as a consequence, under varying gravitational conditions.

Data analysis. For postaerosol inhalation data collected during flight, only the images acquired during the hypergravity phase or in 1G were retained for data analysis. To do so, raw data were used instead of the reconstructed images usually provided by the gamma camera software. A "list mode" file was saved, containing the time (with 1/100-s precision), energy, and *x*- and *y*-position (on a 1024 × 1024 matrix) of each gamma-ray detected by the camera. For the purpose of the present study, four additional signals were acquired in the same file: vertical acceleration via an accelerometer (Dimension Engineering, Akron, OH), respiratory flow via a Fleisch no. 2 pneumotachograph (OEM Medical, Richmond, VA), subject position using a light source and a light-sensitive resistor (Banner Engineering, Minneapolis, MN) to ensure correct position relative to the camera during each imaging session, and an event marker that signaled when radiolabeled particles were generated. Offline analysis of the list mode data was performed with dedicated code using Matlab (Mathworks, Natick, MA). The postprocessing allowed for verification that aerosol delivery was indeed restricted to periods of μG, and that flow and tidal volume were accurately controlled during aerosol inhalation. It also allowed for the exclusion of periods when the subject was moving or misaligned with the position sensor. For the in-flight measurements, data were triaged into three different conditions, μG, 1G, hypergravity, and, as mentioned above, only the events from the 1G or hypergravity conditions were used. Data acquired during the μG phase were discarded, as subjects were more likely to rise up slightly from the seat during μG, despite the use of subject restraints. Data analysis was then performed in the same fashion as in previous studies (19, 20, 42). Only the right lung was used to analyze regional deposition because of the confounding effects of stomach activity on the left side (2, 20). Activity measured at the different time points were decay corrected and normalized by activity measured immediately postaerosol inhalation.

To assess C vs. P deposition, two ROIs were created over the right Co-57 lung image: *1*) a rectangular ROI covering the entire right lung; and *2*) a C ROI, with dimensions equal to one-half the whole lung ROI's width and one-half its height (36). The C region was positioned against the medial boundary of the whole lung region, centered by height, with the P region being the area lying between the central and whole lung outline (Fig. 2*A*). These regions were displayed over the aerosol scans to determine the initial counts in each region. To account for the difference in relative lung area and volume between the two regions, the ratio of C to P counts, $(C/P)_{Tc}$, was normalized by the C/P for the Co-57 scan, $(C/P)_{Co}$. Zeman et al. (43) have shown recently that the transmission scan estimates regional lung volumes similar to that of radiolabeled gas (^{133}Xe) scans in healthy subjects. The resulting C/P provided an index of relative deposition between the two regions. Because the C region outlines both bronchial airways and lung parenchyma around them, a C/P of ≈1 reflects primarily homogenous deposition throughout the pulmonary air spaces. Increases in C/P to values >1 reflect an increase in C vs. P deposition mainly through increased bronchial deposition.

The fraction of activity (corrected for the decay due to the half-life of ^{99m}Tc) remaining in the lung after 22 h, or R_{22}, was used to estimate relative alveolar deposition, assuming negligible alveolar clearance over this period (35) and assuming completion of clearance from the larger ciliated airways. Conversely, $(1 - R_{22})$ was assumed to represent the deposition in the entire tracheobronchial tree where mucociliary clearance is dominant. Furthermore, the clearance of the particles through 90-min postdeposition served as the primary index of relative deposition in the large airways (i.e., $1 - R_{1h30}$); the clearance from 90 min to 4 h postdeposition (i.e., $R_{4h} - R_{1h30}$) was representative of relative deposition in the intermediate airways, while the difference between alveolar deposition and retention at 4 h (i.e., $R_{22} - R_{4h}$) was indicative of relative deposition in the smallest bronchial airways. To assess tracheobronchial retention (TB R_t), i.e., clearance kinetics from only the mucociliary clearance-dependent airways, R_{22} was subtracted from the initial measurements made at 1

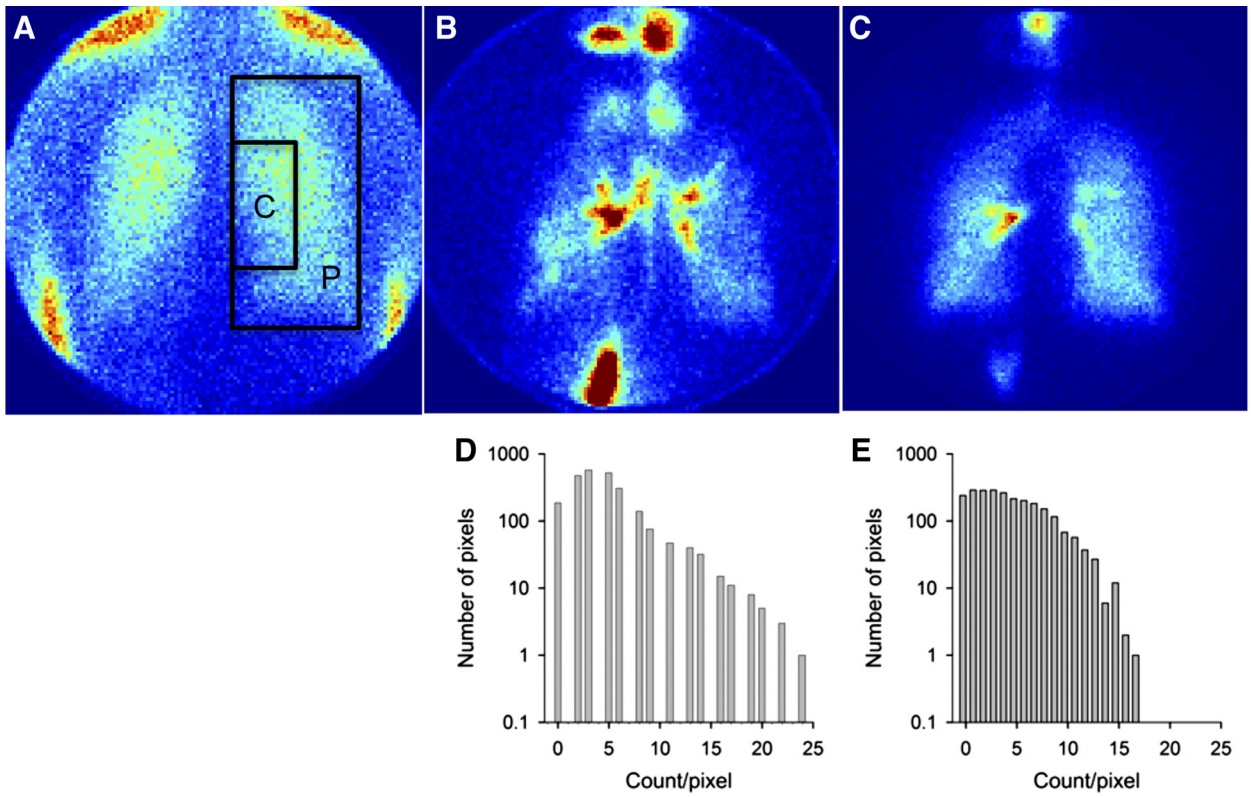

Fig. 2. Gamma scintigraphy images obtained in one subject. *A*: central (C) and peripheral (P) regions of interest were defined based on the transmission scan. Deposition images along with histograms of activity counts from aerosols inhaled in microgravity (μG; *B* and *D*) and on the ground (1G; *C* and *E*) are also shown. Images in *B* and *C* were normalized by the total count in the right lung. The amount of deposition increases from blue to red. Note that, in μG, because of the absence of gravitational sedimentation, fewer particles deposited in the P region than in 1G, leading to significant differences in the histogram distributions.

h 30 min and 4 h postinhalation and normalized by deposition in the bronchial airways (2), i.e.

$$\text{TB } R_t = (R_t - R_{22})/(1 - R_{22})$$

where t = 1 h 30 min or 4 h.

As a further marker of regional deposition, the heterogeneity of aerosol deposition was also determined by the skew (3rd moment about the mean) of the frequency distribution histograms of counts per pixel within the right lung (2, 23). Histograms were obtained from the images acquired immediately postaerosol delivery (Fig. 2, *D* and *E*) by plotting the number of pixels with a given count value (*Y*-axis) as a function of count values (*X*-axis), with the number of pixels being expressed as a fraction of the total number of pixels in the right-lung ROI. The skew of deposition distribution increases with increased frequency of "hot spots," or pixels with counts higher than expected from a normal distribution, in the lung that are presumably due to increased deposition in the bronchial airways (23).

Finally, an analysis similar to that used in the calculation of C/P was performed to determine the ratio of apical (A) to basal (B) deposition, A/B, by vertically dividing the whole lung rectangular region into thirds (apex, middle, and base) (6). As for the C/P, the apex-to-base ratio (A/B) for the deposition images was normalized to the A/B from the Co-57 transmission scan to account for differences in volume associated with each region.

Statistical analysis. All statistical analyses were performed with Systat version 11 (Systat, Evanston, IL). For each experimental condition (gravity level, time point) and for each subject, one single value for retention R_t was determined and used in the statistical analysis. Data were grouped in different categorical variables; G level (μG and 1G), time point (0 h, 1 h 30 min, 4 h, and 22 h), and subject number. A two-way analysis of variance for correlated samples was then performed to test for differences in retention between G level and between time points (see Fig. 4). Post hoc testing using the Bonferroni adjustment was performed for tests showing significant *F*-ratios. Wilcoxon matched-pairs signed-rank tests were used to compare C/P and A/B, skew of deposition distribution, tracheobronchial retention at 1 h 30 min and 4 h, and alveolar retention between gravity levels (see Fig. 3). Significant differences were accepted at the $P < 0.05$ level.

RESULTS

Data were obtained in all but one subject because of hardware problems with aerosol delivery during one of the flights. Thus data are presented for five subjects only. All subjects took anti-motion sickness medication both during flight and during the control studies performed on the ground. The typical number of breaths during each μG phase was six to seven, with aerosol delivery occurring over three to four of these breaths (see Fig. 1*B*). On average, it took subjects 31 breaths in μG and 14 breaths in 1G to reach the intended dose of 40 μCi.

Representative deposition patterns following aerosol inhalation in μG and 1G are presented in Fig. 2 for one subject (deposition increases from blue to red in the color scale), along with a transmission scan showing the C and P ROI for data analysis. Images clearly show that, in μG, most particles deposited centrally with little deposition in the lung periphery. In 1G where gravitational sedimentation was present, a greater proportion of particles deposited in the lung periphery than in μG.

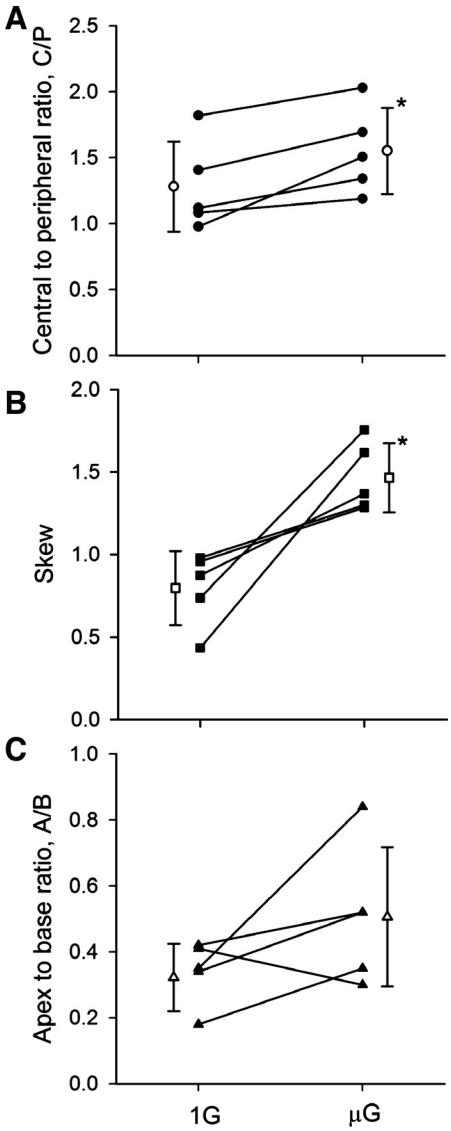

Fig. 3. Deposition indexes for aerosol inhaled in μG and 1G. *A*: C-to-P ratio (C/P). *B*: skew (Sk). *C*: apex-to-base ratio (A/B). Individual data are shown by solid symbols. Data averaged over all subjects (mean ± SD, $n = 5$) are shown by open symbols. *Significantly different from data in 1G ($P < 0.05$).

The effect of gravity level during aerosol inhalation on regional deposition was further assessed in Fig. 3, *A–C*, where the C/P, the skew of the deposition distribution, and the A/B are plotted as a function of G level, respectively. In each panel, data averaged over the five subjects (mean ± SD, open symbols) is shown, as well as individual data (solid symbols), with the latter data illustrating intersubject variability. Compared with inhalation in 1G, all subjects show an increase in C/P (Fig. 3*A*) and skew (Fig. 3*B* and Fig. 2, *D–E*), and four out of five subjects show an increase in A/B (Fig. 3*C*) when particles were inhaled in μG. On average, C/P increased from 1.28 ± 0.34 (mean ± SD) in 1G to 1.57 ± 0.31 in μG ($P = 0.043$), skew increased from 0.80 ± 0.22 in 1G to 1.32 ± 0.19 in μG ($P = 0.043$), and A/B tended to 0.32 ± 0.10 in 1G and to 0.51 ± 0.21 in μG ($P = 0.08$).

The retention of radiolabeled particles that deposited in the right lung and in the tracheobronchial region is shown in Fig. 4, *A* and *B*, respectively, both for particles inhaled in μG (open circles) and in 1G (solid circles). Retention in the C and P region is listed in Table 2. Data show a more rapid decrease in activity for particles inhaled in μG than in 1G, reflecting lower retention for particles that were deposited in the lung during μG. While there was a trend for retention in the P region to be higher than in the C region at 4 and 22 h in both μG and 1G, these differences were not statistically significant with such a small number of subjects (e.g., $P = 0.08$ for C retention vs. P retention at 4 h in 1G).

Figure 5 shows the distribution of deposited particles between the airways (large, intermediate, and small), and the alveolar region (as a percentage of total number of deposited particles). On average, 83% of the particles that deposited in μG did so in the tracheobronchial tree (i.e., $1 - R_{22}$), while only 42% deposited in the same region in 1G.

DISCUSSION

In this study, we used inhalation of ^{99m}Tc-labeled SC particles and gamma scintigraphy to study the effect of gravity on aerosol deposition patterns in healthy adults with normal lung function. Particles were inhaled either in μG or 1G, and retention of deposited particles was monitored during 1G over the 22 h following inhalation. Several indexes were derived from the data to assess regional distribution of deposited particles, all showing significant differences between gravity levels.

Effect of gravity on aerosol deposition patterns. One of the most commonly used indexes is the ratio of deposited particles in the C and P region of the lung (C/P). Because of the 2D

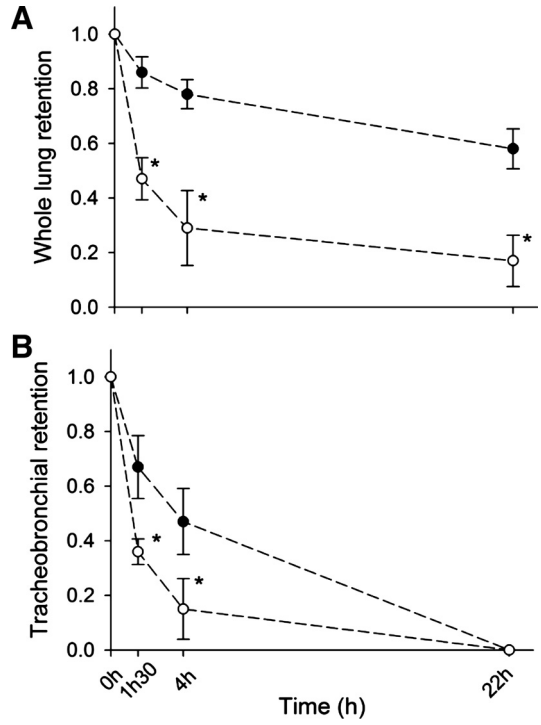

Fig. 4. Retention of radiolabeled particles that deposited in the right lung as a whole (*A*) and in the tracheobronchial region (*B*) as a function of time postinhalation. Data are averaged over all subjects (mean ± SD, $n = 5$). ●, Aerosol inhaled in 1G; ○, aerosol inhaled in μG. *Significantly different compared with 1G data, $P < 0.05$.

Table 2. *Retention of radiolabeled particles in the right lung as a whole and in the central and peripheral region as a function of time postinhalation*

	μG			1G		
Time	Whole lung	C region	P region	Whole lung	C region	P region
0	1	1	1	1	1	1
1 h 30 min	0.47 ± 0.08*	0.50 ± 0.09*	0.45 ± 0.09*	0.86 ± 0.06	0.87 ± 0.10	0.86 ± 0.06
4 h	0.29 ± 0.14*	0.27 ± 0.15*	0.30 ± 0.14*	0.78 ± 0.05	0.72 ± 0.07	0.81 ± 0.06
22 h	0.17 ± 0.09*	0.14 ± 0.04*	0.19 ± 0.14*	0.58 ± 0.07	0.54 ± 0.13	0.60 ± 0.07

Values are means ± SD. μG, microgravity; 1G, gravity on the ground; C, central; P, peripheral. *Significantly different from data in 1G ($P < 0.05$).

nature of our imaging method, the C region defined on our images not only includes the largest conducting airways, but also includes a significant portion of the lung parenchyma. In an adult lung, the volume of the conducting airways (excluding the trachea and extrathoracic upper airway, which were not included in the analysis) is ~100 ml or ~3% of average lung volume during tidal breathing. Thus the C region mainly comprises lung parenchyma. If aerosols deposit uniformly throughout the lungs, the deposition pattern will be expected to be similar to the transmission scan, and the normalized C/P will approach 1.0. Increasing particle deposition in the large airways within the C region will be in addition to the average parenchymal value, raising the C/P above 1. Coarse particles (i.e., ranging between 2.5 and 10 μm) deposit either by inertial impaction, a mechanism most efficient in the large- and medium-sized airways, where airflow velocities are high, or by gravitational sedimentation, which is most efficient in the distal lung, where airway size and airflow velocities are small. Of these two mechanisms, sedimentation is the only gravity-dependent mechanism and is, therefore, affected by the gravitational environment. Our data show that C/P was larger in μG than in 1G, with the ratio increasing from 1.28 in 1G to 1.57 in μG (Fig. 3*A*). In both cases, C/P was larger than unity, i.e., there was significant deposition in the conducting airways. In μG, the absence of gravity caused fewer particles to deposit in the lung periphery than in the central airways, which resulted in a higher C/P than in 1G. It is also possible that, because less particles deposit in the lung periphery in μG, more particles are available for deposition in the central airways during expiration than in 1G. Using a five-lobe model of the human lung that accounted for the influence of gravity, both on airflow distribution and particle deposition, Asgharian and colleagues (1) showed that, while deposition in the alveolar region was reduced in μG compared with 1G, deposition in the conducting airways was unaffected by gravity in the first 10 generations for 1-μm particles and the first 5 generations for 10-μm particles. None of their simulations predicted a larger deposition in the conducting airways in μG, suggesting that deposition by inertial impaction is most effective during inhalation. Therefore, it is very likely that the increase in the C/P in μG results from a decrease in P deposition in the absence of gravity.

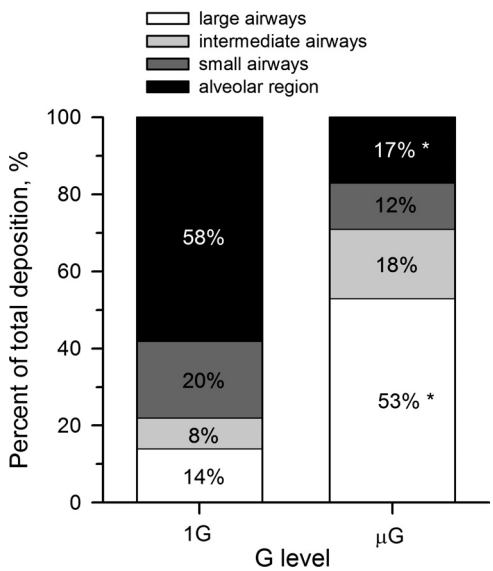

Fig. 5. Effect of gravity on the distribution of deposited particles between the large, intermediate, and small airways, and the alveolar region (black segment). *Significantly different from data in 1G, $P < 0.001$.

The use of the skew of the distribution in analyzing aerosol deposition patterns was first introduced by Garrard et al. (23), who showed that skew was inversely correlated with retention at 24 h, i.e., inversely correlated with alveolar deposition. This observation implies that high values of skew are indicative of deposition occurring predominantly in the bronchial airways, which would be consistent with the presence of hot spots, and low values are associated with deposition occurring mainly in the lung periphery. It should be noted that other factors than deposited particles can produce a skew in the distribution. A skew can be produced simply by the distribution of volume in pixels within the lung, e.g., the skew of the transmission scan is likely nonzero as it represents a 2D image of a 3D lung. However, the changes in skew from μG to 1G should be independent of these other factors and only a function of changing particle deposition within those lung regions. Skew was significantly increased when particles were inhaled in μG compared with 1G (Fig. 3*B* and Fig. 2, *D* and *E*). The increased skew observed in μG results from the presence of "hot spots," likely at bifurcation points due to inertial impaction. In 1G, while still present, these hot spots are somewhat masked by particles that deposit by sedimentation, a process that tends to result in a more homogeneous deposition pattern than for impaction alone. Similar to Garrard et al. (23), we plotted R_{22} for both G levels as a function of skew (Fig. 6) and observed a significant decrease in skew with increasing R_{22}. The lowest values of skew were associated with the largest values of R_{22}, implying that the higher the alveolar deposition, the lower the skew of the distribution, in agreement with previous observations (23).

The distribution of deposited particles among different serial regions of the airways was also assessed by assuming that particles deposited in each of those regions also cleared the

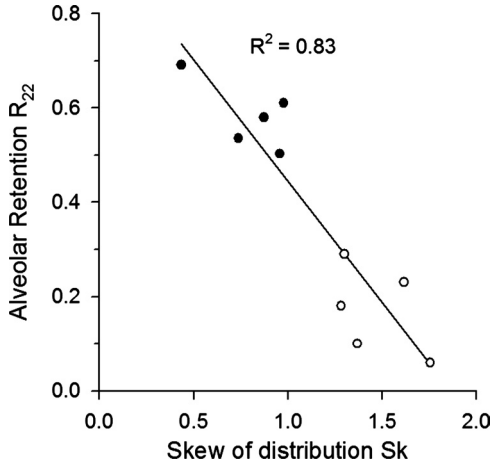

Fig. 6. Regression of alveolar deposition as measured by retention at 22 h (R_{22}) against Sk of distribution for data collected both in μG (○) and in 1G (●).

lung in a serial manner (see Fig. 5). The time points used in this study generally agreed to reflect initial deposition from proximal to distal airways as retention times progress. Clearance from the large airways has been estimated in previous studies by measuring retentions between 1 and 2 h postdeposition, while "24-h retention" measurements have usually been collected 20–24 h postdeposition (2, 26, 42). The additional time point at 4 h allowed us to further distinguish between intermediate and small airways. Based on a previous study in 30 subjects, the 95% confidence interval at each of these data points is expected to be within ±0.05 (3).

Relative alveolar deposition, as estimated by particle R_{22}, was significantly higher in 1G than in μG (Fig. 4*A*), most likely because of significant deposition by gravitational sedimentation in the lung periphery when particles were inhaled in 1G. Also, the majority of particles that deposited in 1G did so in the alveolar region, while particles that deposited in μG were predominantly located in the larger airways where inertial impaction is expected to be the most efficient (Fig. 5). In a previous study of aerosol deposition in μG (12), Darquenne et al. (10) used a one-dimensional model of aerosol transport in the lung to predict the contribution of the mechanisms of inertial impaction, gravitational sedimentation, and Brownian diffusion to aerosol deposition. In 1G, deposition of 0.5- to 3-μm-diameter particles was mainly due to gravitational sedimentation and, to a lesser extent, to inertial impaction with minimal contribution of Brownian diffusion. In μG, when sedimentation was removed, deposition occurred through a combination of Brownian diffusion in the lung periphery and inertial impaction in the conducting airways with Brownian diffusion accounting for 100, 92, 47, and 25% of the total number of deposited particles for 0.5-, 1-, 2-, and 3-μm-diameter particles, respectively. This decrease in the contribution of Brownian diffusion to overall deposition can be approximated by an exponential decrease ($R^2 = 0.98$). While that previous study did not use 5-μm-diameter particles, extrapolating the exponential fit to 5-μm particles predicts a diffusive contribution of 8% to total deposition, i.e., ~50% of the R_{22} measured in our experiments. Also, despite having subjects breathe out to residual volume at the end of each μG period during aerosol exposure (Fig. 1*B*), it is possible that some particles that penetrate in the lung periphery were not exhaled and subsequently deposited during the hypergravity portion of the parabola, also contributing to the nonzero R_{22}. Furthermore, the presence of fine particles in the polydisperse aerosol may have resulted in P deposition by diffusion; however, because the amount of radiolabel is proportional to particle size, the contribution from small particles to measured retention is expected to be small. Finally, it should be noted that there has been debate over the past 20 yr as to the degree to which 24-h retention reflects initial alveolar deposition vs. some residual bronchial airway deposition. In other words, it may be that not all particles deposited in the bronchial airways are cleared by 24 h postdeposition (4, 28, 40). If this was the case, then our data in μG (Fig. 5) suggest that as much as 17% of particles residing in bronchial airways may not be cleared during the initial 24 h postdeposition. Interestingly, this R_{22} (17%) is similar to that found by Camner et al. (7) (16% at 24 h) for inhalation of 10-μm particles under tidal breathing conditions at a very low flow rate. They also concluded that, by modeling considerations, their particles should have been deposited entirely in the bronchial airways, suggesting a residual retention in these airways beyond 24 h. Nevertheless, no matter what mechanism is responsible for the nonzero R_{22} measured in μG, it does not alter the fact that *1*) the C/P is significantly higher (Fig. 3) and *2*) retentions in all regions are significantly lower (Table 2) for particles deposited in μG vs. particles deposited in 1G, strongly suggesting a shift in relative deposition toward the bronchial airways in the absence of gravity.

The distribution of deposited particles between the apex and the base of the lung was assessed by the A/B (Fig. 3*C*). For the particle size range and flow rate used in this study, inhaled particles are likely to follow the distribution of flow at least down to the level of the segmental bronchi. Indeed, in a modeling study, Darquenne et al. (15) have shown that the delivery of inhaled particles to the lung segments was dominated by convective flow for specific breathing conditions and particle sizes, which could be characterized by a single parameter, the Stokes' number. Their predictions suggested that, when the Stokes number in the trachea was <0.01, aerosol and gas flow were proportionally distributed to the lung segments. Similar conclusions can be derived from the work of de Vasconcelos et al. (18), where the importance of the Stokes number on characterizing aerosol transport through airway bifurcations was also highlighted. Assuming a tracheal diameter of 1.8 cm and a flow rate of 0.5 l/s, the Stokes' number in the trachea is <0.01 for particles up to a diameter of 5.5 μm (8). Because the lung distorts under its own weight, the alveoli at the bottom (base) of the lung are more compressed than the alveoli at the top (apex), and, because poorly expanded alveoli are more compliant, ventilation is greatest near the bottom of the lung and becomes gradually lower toward the top of the lung. These variations in regional ventilation affect the transport and deposition of inhaled particles, with more particles being delivered to the base of the lung than the apex in 1G. These regional differences are largely reduced in μG (25, 38), and, therefore, one might expect a more uniform deposition pattern over the lung height, which would be reflected in a larger A/B in μG than in 1G. Although not significant, our data show a trend in that direction, with four out of five subjects having an increase in the A/B when particles were inhaled in μG compared with 1G (Fig. 3*C*).

Relevance to extraterrestrial exploration. Estimating the risk of lunar or Martian dust to the lung involves three key aspects. First is the nature of the dust itself. Data suggest that both the lunar and Martian dusts have properties that make them potentially hazardous (29–31). Second is the amount of deposition of the dust that is inhaled. Third is how long the dust that does deposit remains in the lung and so is available to potentially cause damage. These last two aspects are addressed in this study. While the effect of μG on mucociliary clearance and alveolar macrophage phagocytosis is unknown (31), it is likely that, even in μG, mucociliary clearance is a faster mechanism than phagocytosis by alveolar macrophages. Therefore, if insoluble particles are deposited more peripherally in μG than in 1G, they will not be in a position to be as readily cleared by the mucociliary clearance system, thus increasing their residence time in the lungs. Conversely, if particles were to be mainly deposited centrally in the absence of gravity, their residence time in the lungs would be reduced. For coarse particles (~5 μm), our data strongly suggest that, in low gravity, most of the deposited particles are located in the airways (83 vs. 17% in the lung periphery). As a consequence, they are readily cleared by the lungs, minimizing any potential toxicological effect they might have. Therefore, toxicological studies performed on the ground for particles in the coarse range would provide an upper limit of potential effects of inhaled particulates to the health of future human explorers to other planetary objects for these sized particles. Because this study utilized only coarse particles, the question of the site of deposition of fine particles in a reduced gravity environment remains unanswered. Recent data in animals, however, suggest a more P deposition of fine particles in μG than in 1G. Recently, Darquenne and colleagues (9) delivered aerosolized 0.9-μm-diameter particles to spontaneously breathing rats both in μG and 1G and measured aerosol deposition in these animals using postmortem magnetic resonance imaging techniques. They showed a reduced C/P in μG compatible with an increase in the contribution of P deposition to overall deposition.

Limitations. To quantify particle deposition in the lung, a reference image is required to define ROIs and to normalize deposition to lung thickness. This is because deposition patterns may not cover the whole lung, and, therefore, patterns obtained by 2D gamma scintigraphy do not necessarily coincide with the actual boundary of the lungs. The reference image is usually obtained with a gas ventilation scan (^{133}Xe or ^{81}Kr) or, in some cases, with a transmission scan (^{57}Co or ^{99m}Tc), as in this study. Both approaches have their pros and cons (43). In a ventilation scan, the radioactive gas filling the lungs yields an image with pixel counts nearly proportional to the thickness of the lung. However, poorly ventilated regions of the lung may be underevaluated as the inhaled radioactive gas will not fully equilibrate within these lung regions. A transmission scan produces a density image through the entire thickness of the chest that is proportional to the density of the tissue through which it attenuates and is independent of regional ventilation deficiencies. However, transmission scans are affected by attenuation through both the anterior and posterior tissues of the chest, whereas measurements of deposited radiolabeled particles are only attenuated by the posterior tissues of the chest, as the subjects are typically sitting with their back to the camera. Zeman and colleagues (43) recently compared deposition patterns using 2D gamma scintigraphy, where data were normalized either to a ^{99m}Tc transmission scan or a ^{133}Xe ventilation scan. Although normalized C/P were significantly smaller for the ventilation scan method than the transmission scan method, the correlation of normalized C/P between the two methods was strong. This suggests that both methods give reliable measures of C/P.

The shape and size of the lung is influenced by gravity, which may affect the analysis of data collected during parabolic flight. Previous lung studies during parabolic flights suggest that this effect may be minimal. Indeed, although there is a small change in resting lung volume in low gravity (21), radiographic studies in parabolic flight have shown that lung margins and shape change only minimally in μG (33). While these radiographic studies did not look at the effect of hypergravity on the lung, a study by Paiva et al. (37) showed only a small increase in functional residual capacity of ~200 ml and a slightly larger contribution of the diaphragm during tidal breathing in 2G compared with 1G. As only data collected during 1G and the hypergravity phase of the parabolas were used in the data analysis, it is unlikely that the small changes in lung volumes between these gravity levels have significantly affected the results. Similarly, it appeared that the effect of changes in lung tissue distribution between 1G and hypergravity also had a minimal effect on calculated parameters. Indeed, comparison between calculated values of C/P, skew, and A/B using only data collected in 1G or in hypergravity differed by <5%.

Finally, there was a small difference in the particle size generated by the Aeroneb when operated during flight and on the ground. The Aeroneb produced a slightly larger MMAD in μG than in 1G (5.6 vs. 4.9 μm), but with a similar GSD. The smaller size measured at 1G is possibly due to the increased loss of the largest particles due to settling along the path to the cascade impactor (i.e., measurement artifact) and/or to small changes in the separation force of the droplets from the vibrating mesh (i.e., true difference in inspired aerosol). Reference values for lung deposition during mouth breathing (in 1G) at a similar flow rate as that used in this study indicate a total deposition of 71% for 5-μm particles and 74% for 7-μm particle (27). Given the similar deposition values and given similar GSD of the produced aerosol at both G level, it is unlikely that the difference in the output size of the Aeroneb has significantly affected our data.

In summary, this study reports the effect of gravity on the deposition patterns of coarse particles (~5 μm) in the human lung. Deposition and retention of particles were determined by planar gamma scintigraphy immediately following particle inhalation, and up to 22 h postdeposition. All indexes of deposition show a significant effect of gravity on aerosol deposition. In particular, the data show a profound shift in the relative distribution of deposited particles away from the lung periphery toward the large airways when particles were inhaled in μG. This is the direct result of a decrease in P deposition in the absence of gravitational sedimentation rather than an increase in C deposition.

ACKNOWLEDGMENTS

We acknowledge the technical support of Michael Chose and Frank Rüdiger at MiE, and of Wanda Thompson, Dominic Del Rosso, and the reduced gravity office at National Aeronautics and Space Administration-

Johnson Space Center (NASA-JSC). We are also grateful for the medical support of Drs. William Carpentier and James Locke at NASA-JSC.

GRANTS

This work was supported by the National Space Biomedical Research Institute through NASA NCC 9-58 (Grant HFP01604).

DISCLOSURES

No conflicts of interest, financial or otherwise, are declared by the author(s).

AUTHOR CONTRIBUTIONS

Author contributions: C.D., W.D.B., and G.K.P. conception and design of research; C.D., K.L.Z., R.C.S., T.K.C., J.M.F., W.D.B., and G.K.P. performed experiments; C.D., K.L.Z., R.C.S., T.K.C., J.M.F., and W.D.B. analyzed data; C.D., K.L.Z., R.C.S., W.D.B., and G.K.P. interpreted results of experiments; C.D. prepared figures; C.D. drafted manuscript; C.D., K.L.Z., R.C.S., T.K.C., J.M.F., W.D.B., and G.K.P. edited and revised manuscript; C.D., K.L.Z., R.C.S., T.K.C., J.M.F., W.D.B., and G.K.P. approved final version of manuscript.

REFERENCES

1. **Asgharian B, Price OT, Oberdorster G.** The effect of gravity on airflow distribution and particle deposition in the lung. *Inhal Toxicol* 18: 473–481, 2006.
2. **Bennett WD, Herbst M, Alexis NE, Zeman KL, Wu J, Hernandez ML, Peden DB.** Effect of inhaled dust mite allergen on regional particle deposition and mucociliary clearance in allergic asthmatics. *Clin Experim Allergy* 41: 1719–1728, 2011.
3. **Bennett WD, Laube BL, Corcoran T, Zeman K, Sharpless G, Thomas K, Wu J, Mogayzel PJ, Pilewski J, Donaldson S.** Multisite comparison of mucociliary and cough clearance measures using standardized methods. *J Aerosol Med Pulm Drug Deliv* 26: 157–164, 2013.
4. **Bennett WD, Scheuch G, Zeman KL, Brown JS, Kim CS, Heyder J, Stahlhofen W.** Bronchial airway deposition and retention of particles in inhaled boluses: effect of anatomic dead space. *J Appl Physiol* 85: 685–694, 1998.
5. **Bennett WD, Scheuch G, Zeman KL, Brown JS, Kim CS, Heyder J, Stahlhofen W.** Regional deposition and retention of particles in shallow, inhaled boluses: effect of lung volume. *J Appl Physiol* 86: 168–173, 1999.
6. **Brown JS, Zeman KL, Bennett WD.** Regional deposition of coarse particles and ventilation distribution in healthy subjects and patients with cystic fibrosis. *J Aerosol Med* 14: 443–454, 2001.
7. **Camner P, Anderson M, Philipson K, Bailey A, Hashish A, Jarvis N, Bailey M, Svartengren M.** Human bronchiolar deposition and retention of 6-, 8- and 10-μm particles. *Exp Lung Res* 23: 517–535, 1997.
8. **Darquenne C.** Aerosol deposition in health and disease. *J Aerosol Med Pulm Drug Deliv* 25: 140–147, 2012.
9. **Darquenne C, Borja MG, Oakes JM, Breen EC, Olfert IM, Scadeng M, Prisk GK.** Central to peripheral deposition ratio of inhaled aerosols is less in microgravity than in normal gravity. *Am J Resp Crit Care Med* 185: A5587, 2012.
10. **Darquenne C, Paiva M.** One-dimensional simulation of aerosol transport and deposition in the human lung. *J Appl Physiol* 77: 2889–2898, 1994.
11. **Darquenne C, Paiva M, Prisk GK.** Effect of gravity on aerosol dispersion and deposition in the human lung after periods of breath-holding. *J Appl Physiol* 89: 1787–1792, 2000.
12. **Darquenne C, Paiva M, West JB, Prisk GK.** Effect of microgravity and hypergravity on deposition of 0.5- to 3-μm-diameter aerosol in the human lung. *J Appl Physiol* 83: 2029–2036, 1997.
13. **Darquenne C, Prisk GK.** Aerosol deposition in the human respiratory tract breathing air and 80:20 heliox. *J Aerosol Med* 17: 278–285, 2004.
14. **Darquenne C, Prisk GK.** Deposition of inhaled particles in the human lung is more peripheral in lunar than in normal gravity. *Eur J Appl Physiol* 103: 687–695, 2008.
15. **Darquenne C, van Ertbruggen C, Prisk GK.** Convective flow dominates aerosol delivery to the lung segments. *J Appl Physiol* 111: 48–54, 2011.
16. **Darquenne C, West JB, Prisk GK.** Deposition and dispersion of 1 μm aerosol boluses in the human lung: effect of micro- and hypergravity. *J Appl Physiol* 85: 1252–1259, 1998.
17. **Darquenne C, West JB, Prisk GK.** Dispersion of 0.5–2μm aerosol in micro- and hypergravity as a probe of convective inhomogeneity in the human lung. *J Appl Physiol* 86: 1402–1409, 1999.
18. **de Vasconcelos TF, Sapoval B, Andrade JS, Grotberg JB, Filoche M.** Particle capture into the lung made simple? *J Appl Physiol* 110: 1664–1673, 2011.
19. **Donaldson SH, Bennett WD, Zeman KL, Knowles MR, Tarran R, Boucher RC.** Mucus clearance and lung function in cystic fibrosis with hypertonic saline. *New Engl J Med* 354: 241–250, 2006.
20. **Donaldson SH, Corcoran TE, Laube BL, Bennett WD.** Mucociliary clearance as an outcome measure for cystic fibrosis clinical research. *Proc Am Thorac Soc* 4: 399–405, 2007.
21. **Elliott AR, Prisk GK, Guy HJB, West JB.** Lung volumes during sustained microgravity on spacelab SLS-1. *J Appl Physiol* 77: 2005–2014, 1994.
22. **Foster WM.** Is 24 hour lung retention an index of alveolar deposition? *J Aerosol Med* 1: 1–10, 1988.
23. **Garrard CS, Gerrity TR, Schreiner JF, Yeates DB.** The characterization of radioaerosol deposition in the healthy lung by histogram distribution analysis. *Chest* 80: 840–842, 1981.
24. **Graf JC.** *Lunar Soils Grain Size Catalog*. Washington, DC: NASA, 1993. (Publ. NASA-RP-1265)
25. **Guy HJB, Prisk GK, Elliott AR, Deutschman RA III, West JB.** Inhomogeneity of pulmonary ventilation during sustained microgravity as determined by single-breath washouts. *J Appl Physiol* 76: 1719–1729, 1994.
26. **ICRP.** Human respiratory tract model for radiological protection: a report of the task group of the International Commission on Radiological Protection. ICRP Publication 66 Annexe D (Deposition of inhaled particles). *Ann ICRP* 24: 231–299, 1994.
27. **ICRP.** Human respiratory tract model for radiological protection: a report of the task group of the International Commission on Radiological Protection. ICRP Publication 66 Annexe F (Reference values for regional deposition). *Ann ICRP* 24: 415–432, 1994.
28. **Ilowite JS, Smaldone GC, Perry RJ, Bennett WD, Foster WM.** Relationship between tracheobronchial particle clearance rates and sites of initial deposition in man. *Arch Environ Health* 44: 267–273, 1989.
29. **Lam CW, James JT, Latch JN, Hamilton RF Jr, Holian A.** Pulmonary toxicity of simulated lunar and Martian dusts in mice. II. Biomarkers of acute responses after intratracheal instillation. *Inhal Toxicol* 14: 917–928, 2002.
30. **Lam CW, James JT, McCluskey R, Cowper S, Balis J, Muro-Cacho C.** Pulmonary toxicity of simulated lunar and Martian dusts in mice. I. Histopathology 7 and 90 days after intratracheal instillation. *Inhal Toxicol* 14: 901–916, 2002.
31. **Linnarsson D, Carpenter J, Fubini B, Gerde P, Karlsson LL, Loftus DJ, Prisk GK, Staufer U, Tranfield EM, van Westrenen W.** Toxicity of lunar dust. *Planetary and Space Science* 74: 57–71, 2012.
32. **Ma B, Darquenne C.** Aerosol deposition characteristics in distal acinar airways under cyclic breathing conditions. *J Appl Physiol* 110: 1271–1282, 2011.
33. **Michels DB, Friedman PJ, West JB.** Radiographic comparison of human lung shape during normal gravity and weightlessness. *J Appl Physiol* 47: 851–857, 1979.
34. **Moller W, Haussinger K, Winkler-Heil R, Stahlhofen W, Meyer T, Hofmann W, Heyder J.** Mucociliary and long-term particle clearance in the airways of healthy nonsmoker subjects. *J Appl Physiol* 97: 2200–2206, 2004.
35. **Mortensen J, Lange P, Nyboe J, Groth S.** Lung mucociliary clearance. *Eur J Nucl Med* 21: 953–961, 1994.
36. **Newman S, Bennett WD, Biddiscombe M, Devadason SG, Dolovich MB, Fleming G, Haeussermann S, Kietzig C, Kuelh PJ, Laube BL, Sommerer K, Taylor G, Usmani OS, Zeman KL.** Standardization of techniques for using planar (2D) imaging for aerosol deposition assessment of orally inhaled products. *J Aerosol Med Pulm Drug Deliv* 25, *Suppl* 1: S10–S28, 2012.
37. **Paiva M, Estenne M, Engel LA.** Lung volumes, chest wall configuration, and pattern of breathing in microgravity. *J Appl Physiol* 67: 1542–1550, 1989.
38. **Prisk GK, Guy HJB, Elliott AR, Paiva M, West JB.** Ventilatory inhomogeneity determined from multiple-breath washouts during sustained microgravity on Spacelab SLS-1. *J Appl Physiol* 78: 597–607, 1995.

39. **Scheuch G, Stahlhofen W, Heyder J.** An approach to deposition and clearance measurements in human airways. *J Aerosol Med* 9: 35–41, 1996.
40. **Smaldone GC, Perry RJ, Bennett WD, Messina MS, Zwang J, Ilowite JS.** Interpretation of "24 hour lung retention" in studies of mucociliary clearance. *J Aerosol Med* 1: 11–20, 1988.
41. **Stahlhofen W, Gebhart J, Heyder J.** Experimental determination of the regional deposition of aerosol particles in the human respiratory tract. *Am Ind Hyg Assoc J* 41: 385–398, 1980.
42. **Zeman KL, Wu J, Bennett WD.** Targeting aerosolized drugs to the conducting airways using very large particles and extremely slow inhalations. *J Aerosol Med Pulm Drug Deliv* 23: 363–369, 2010.
43. **Zeman KL, Wu J, Donaldson SH, Bennett WD.** Comparison of ^{133}Xenon ventilation equilibrium scan (XV) and ^{99m}Technetium transmission (TT) scan for use in regional lung analysis by 2D gamma scintigraphy in healthy and cystic fibrosis lungs. *J Aerosol Med Pulm Drug Deliv* 26: 94–100, 2013.